REPORT DOCUMENTATION PAGE

Form Approved OMB NO. 0704-0188

1. REPORT DATE (DD-MM-YYYY)	2. REPORT TYPE	3. DATES COVERED (From - To)
29-08-2023	Final Report	1-May-2021 - 30-Apr-2023

4. TITLE AND SUBTITLE
Final Report: Virtual Substrate Simulation

5a. CONTRACT NUMBER
W911NF-21-2-0115

5b. GRANT NUMBER

5c. PROGRAM ELEMENT NUMBER
611102

6. AUTHORS

5d. PROJECT NUMBER

5e. TASK NUMBER

5f. WORK UNIT NUMBER

7. PERFORMING ORGANIZATION NAMES AND ADDRESSES

Boston University
Office of Sponsored Program
881 Commonwealth Avenue
Boston, MA 02215 -1300

8. PERFORMING ORGANIZATION REPORT NUMBER

9. SPONSORING/MONITORING AGENCY NAME(S) AND ADDRESS (ES)

U.S. Army Research Office
P.O. Box 12211
Research Triangle Park, NC 27709-2211

10. SPONSOR/MONITOR'S ACRONYM(S)
ARO

11. SPONSOR/MONITOR'S REPORT NUMBER(S)
78595-PE.2

12. DISTRIBUTION AVAILIBILITY STATEMENT

Approved for public release; distribution is unlimited.

13. SUPPLEMENTARY NOTES

The views, opinions and/or findings contained in this report are those of the author(s) and should not contrued as an official Department of the Army position, policy or decision, unless so designated by other documentation.

14. ABSTRACT

15. SUBJECT TERMS

16. SECURITY CLASSIFICATION OF:			17. LIMITATION OF ABSTRACT	15. NUMBER OF PAGES	19a. NAME OF RESPONSIBLE PERSON
a. REPORT	b. ABSTRACT	c. THIS PAGE			Enrico Bellotti
UU	UU	UU	UU		19b. TELEPHONE NUMBER 617-516-7965

RPPR Final Report
as of 31-Aug-2023

Agency Code: 21XD

Proposal Number: 78595PE **Agreement Number: W911NF-21-2-0115**
INVESTIGATOR(S):

Name: Ph.D. Enrico Bellotti
Email: bellotti@bu.edu
Phone Number: 6175167965
Principal: Y

Name: Dmitry Bedrov
Email: d.bedrov@utah.edu
Phone Number: 8015853949
Principal: N

Organization: **Boston University**
Address: Office of Sponsored Program, Boston, MA 022151300
Country: USA
DUNS Number: 049435266 EIN: 042103547

Report Date: 31-Jul-2023 Date Received: 29-Aug-2023
Final Report for Period Beginning 01-May-2021 and Ending 30-Apr-2023
Title: Virtual Substrate Simulation
Begin Performance Period: 01-May-2021 **End Performance Period:** 30-Apr-2023
Report Term: 0-Other

Submitted By: Ph.D. Enrico Bellotti Email: bellotti@bu.edu
Phone: (617) 516-7965

STEM Degrees: **STEM Participants:**

Major Goals: The goal of the proposed program is to use appropriate numerical simulation approaches to understand the physical mechanisms that control the growth of InGaSb (InGaAlSb) graded layers, for a specific lattice constant, and make them suitable for growth of high quality SLs, and for alloy architectures. Specifically, we are interested in determining if there is an optimum grading profile that leads to a minimum areal dislocation density at the surface of the graded layer that constitute the virtual substrate

Accomplishments: The major accomplishment of the program were:

- Developed they alloy model for InGaSb using density functional theory.

- Developed a validated force field for InGaSb to be used for molecular dynamics simulation.

- Develop a molecular dynamics model for GaSb and InSb and used to simulate the growth of InGaSb films on GaSb. The mechanism of growth and techniques for matching the simulation speed with the actual physical deposition rate where also investigated.

- The nature of defects created during growth was also investigated and the mechanism responsible for creating the defects identified.

- The dislocation structure and evolution was investigate for relevant InGaSb films.

Training Opportunities: Nothing to Report

Results Dissemination: We have not published any manuscripts as a result of this program.
Dr. Bedrov presented the work at the 2023 CSM Annual Meeting.

Honors and Awards: Nothing to Report

RPPR Final Report
as of 31-Aug-2023

Protocol Activity Status:

Technology Transfer: Nothing to Report

PARTICIPANTS:

Participant Type: Postdoctoral (scholar, fellow or other postdoctoral position)
Participant: Alex Kyrtsos
Person Months Worked: 1.00 **Funding Support:**
Project Contribution:
National Academy Member: N

Participant Type: Co-Investigator
Participant: Justin Hooper
Person Months Worked: 6.00 **Funding Support:**
Project Contribution:
National Academy Member: N

Participant Type: Co PD/PI
Participant: Dmitry Bedrov
Person Months Worked: 1.00 **Funding Support:**
Project Contribution:
National Academy Member: N

Partners

,

I certify that the information in the report is complete and accurate:
Signature: Enrico Bellotti
Signature Date: 8/29/23 9:54PM

Multiscale modeling tools for defects optimization in virtual substrates

Dmitry Bedrov
Department of Materials Science & Engineering
University of Utah

Enrico Bellotti
Electrical and Computer Engineering Department and Material Science Program
Boston University

Dr. Tania M. Paskova
Program Manager
Electronic Sensing
CCDC ARL - Army Research Office
tania.m.paskova.civ@mail.mil
919-549-4334

Contract Number W911NF-21-2-0115

1. Force fields for InGaSb

Initial potentials were taken from the work done by Ciani et. al. [1] where they were developed specifically to apply to semiconductor involving the quaternary system of interest investigated herein. Since the potentials were not explicitly verified for the binary and ternary mixtures employed in our simulations, we performed verification of the potentials against DFT data. The potentials were found to perform excellently with respect to reproducing the observed systematic energies as a function of crystal unit cell composition and extent of compression.

2. Molecular Dynamics Simulations

2.1. Establishing deposition protocol

In order to simulate the MBE process, we employ the LAMMPS molecular dynamics simulation package.[2] At this point in its development, LAMMPS is a multifunctional suite of interacting simulation techniques which are accessed by a somewhat rudimentary "scripting language" which allows access to performing sophisticated simulation protocols in a compositional approach by implementing multiple operations in proscribed sub-blocks and orders. For the work discussed herein, the general composition of the simulations is as follows:

I. Construct a substrate layer of GaSb exactly 3 unit cells in height by placing the appropriate atoms on exact lattice locations corresponding to the inherent GaSb zincblende crystal structure (The substrate surface is chosen along a (001) intersection plane, mimicking experiment)

II. Equilibrate the GaSb substrate for 10ns, sufficient time to allow for surface reordering and structure relaxation commensurate with this reordering

III. Deposit "integral" layers of $Ga_xIn_{1-x}Sb$ to build the active material atop the underlying substrate

Step III is the point where the sophistication of the simulation comes into play. The LAMMPS deposition capabilities allow for the insertion of atoms or molecules into the simulation with prescription of velocity, deposition position, deposition rate, and other variables all of which are specified by the user. Simulations are performed in a "layerwise" fashion, where we necessarily define a layer as the total of atoms which would provide the necessary mass to build a single layer spanning the cross-sectional area of the perfect substrate exactly one unit cell thick, at the current composition being deposited. It is important to understand that this does not actually generate a uniform, single unit cell layer of crystal across the underlying substrate, due to both the thermodynamics and kinetics involved in simulation of the system.

Deposition simulations inject atoms periodically from an origination location that is randomly chosen in a plane parallel to the substrate surface with at least 20 angstroms of space between the highest point on the crystal surface as of the last deposited "layer". Atoms are injected concurrently at a rate appropriate for the overall composition of the system. Notably, this means that the simulation protocol injects the type III/V atoms *concurrently* rather than building them

up one monolayer at a time. For most nonzero concentrations of In, the net effect of this scheme is still the injection of a single atom at a time, generally with many picoseconds between injection events. In cases where there are integral multiples of In to Ga as well as these multiples sharing a common multiplicative factor with the rate of deposition of Sb, situations may arise where two atoms are injected at the same time. However, even in such cases, the chances of two atoms being introduced concurrently within interaction range of each other is inversely related to the cross-sectional area of the substrate. Practically, this means that across many microseconds of total simulation time, we have never observed interactions between any atoms before encountering the surface.

Initial simulations were performed using this scheme, with an initial deposition surface of 5 unit

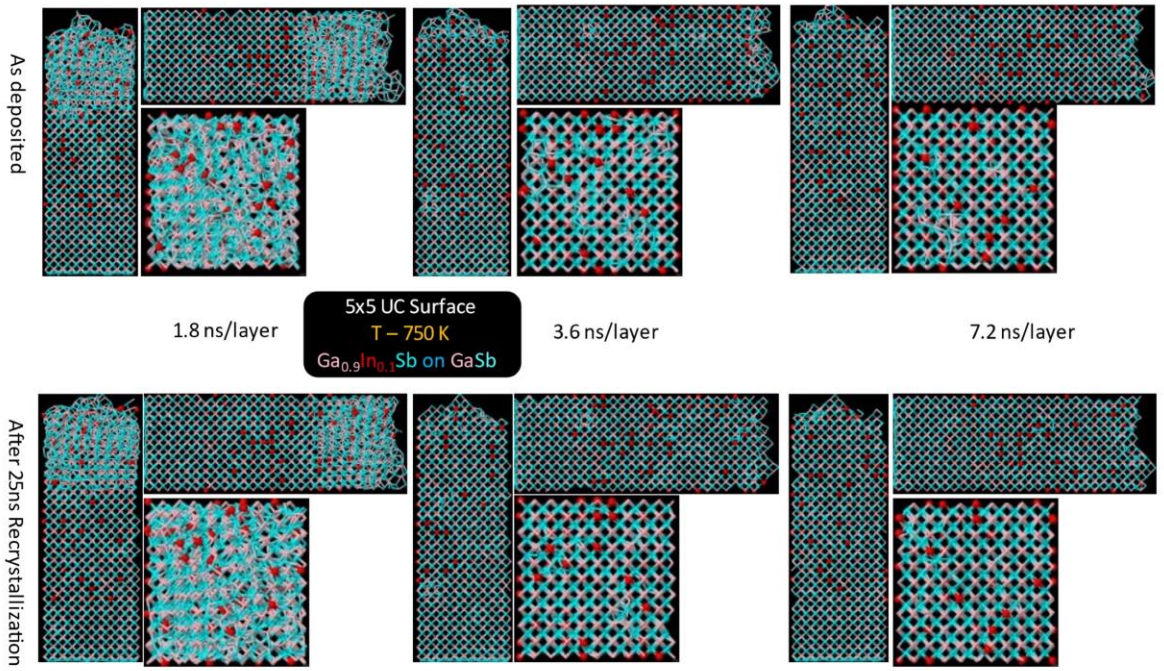

Figure 1: *Comparison of crystal structures for various deposition speeds of 10 layers of $Ga_{0.9}In_{0.1}Sb$ deposited atop 3 layers of GaSb perfect substrate crystal.*

cells (UC) in each of the planar directions, largely to establish the validity of the simulation regime and investigate the performance of the deposition protocol in a simulation environment where rapid result iteration was possible, as simulation time scales (at best) linearly with the overall size (number of atoms) in the simulated system. Figure 1 presents a series of results from simulations of such a system, where 10 layers of $Ga_{0.9}In_{0.1}Sb$ were deposited atop the 3 layer deep, (001) oriented GaSb substrate, with the entire system being simulated at 750K. Indium atoms are depicted as large red spheres in Figure 1 to highlight their presence and distribution within the system, while Ga simulation sites have pink bonds extending from them and Sb sites have cyan bonds extending from them. As can be seen, with a 5x5 UC cross-section, there is a strong cutoff between depositing layers “fast” and “slow”, where for this size of cross-sectional area the cutoff between the two would seem to fall somewhere between 1.8ns/layer and 3.6ns/layer. In the 1.8ns/layer rate, at some point in the latter layers of deposition, lattice disruption occurs faster

than relaxation can occur, leading to the global growth of a disrupted top lattice within the system and corruption of the underlying crystal system. The bottom half of Figure 1 displays the same results after a 25ns recrystallization period, in which the systems were held at the same 750K temperature and allowed to equilibrate or 'recrystallize' for an additional 25 ns. As can be seen in comparing the 1.8ns/layer and 3.6 ns/layer systems, such a recrystallization has some effect on yielding a more regular crystal structure if the area of initial disruption Is relatively close to the surface, where relaxation can take place. For the 1.8 ns/layer system, the disruption extends deeply into the system and as such is unable to relax significantly. In comparison, the 3.6 ns/layer system initially has a bit of surface disruption which subsequently is relaxed out by the recrystallization simulation. However, looking farther toward the substrate of the 3.6 ns/layer system, it can be seen that embedded lattice defects are again largely unable to relax through recrystallization, most likely due to the effect of the surrounding atoms casting the localized misalignment into a deep relative thermodynamic well which would require long range motion of the lattice to move the defect to the surface.

It is worth noting that we attempted multiple longer relaxation runs for the 1.8 ns/layer system to see if we simply had not given the crystal enough time to relax, but the results showed no substantial difference. It is important to note that in *all* of the simulations performed here, the deposition rates are accelerated over what is seen experimentally. This is by necessity, experimental rates of growth are on the order of maximum speeds of a micron per hour. In simulation relevant scales, this represents roughly 2×10^9 ns/layer, or roughly 9 orders of magnitude slower. At this point, it should also be pointed out that we do not know for these types of systems, a priori, whether the defects seen remaining in the 3.6 ns/layer or even the 7.2 ns/layer system represent kinetically formed defects (because we have deposited too quickly and stuck the crystal structure in a metastable configuration) or equilibrium formed defects (due to the defected structure actually representing the lowest free energy of the system).

One final observation was made regarding the 5x5 UC simulation samples: It was observed when investigating the formation of the layers during the deposition process that one of two end states tended to be observed: A nearly correct crystal system with only a few point defects within the lattice (at worst; often these quickly disappeared as deposition progressed) or a completely defected crystal structure (as in the 1.8 ns/layer system). No simulation was noted, across multiple instantiations and intermediate rates, with a localized but persistent dislocation within the system. This essentially points to the conclusion that a 5x5 UC cell is likely too small, laterally, to stabilize the presence of an isolated dislocation. For this reason, became necessary to investigate larger unit cells.

2.2. Elucidating the nature of the observed defects

Figure 2 presents a comparison of the same deposition regime as that of Figure 1, with the sole exception being that the lateral substrate basis upon which the layers are deposited has been expanded to be 15x15 UC cross-section. Here, similar effects can be seen when compared to the smaller surface in terms of the formation retention of defects/dislocations in the lattice, despite the increased size of the substrate base. However, at the same time, the larger substrate base

does allow for the formation of a partially dislocated crystallite in the 1.8 ns/layer deposition rate system, which again persists (albeit with a lessened prominence) after the recrystallization simulation. This points to defects in the fastest layer deposition speed being due to kinetic effects, but without the ability to fully equilibrate.

In order to try to disambiguate this question, we simulated additional systems with deposition of 10 layers of pure GaSb atop the underlying GaSb substrate as well as deposition of 10 layers of pure InSb atop the underlying GaSb substrate at the slowest rate, to ascertain whether or not there was spurious stabilization of crystalline systems which shouldn't be occurring during deposition. In the former system, we know that the fully ordered lattice is the lowest energy system, while we expect the presence of significant defects throughout the crystal for the pure InSb systems to be an energetic, rather than kinetic, outcome, and the presence of an undisrupted crystal in this

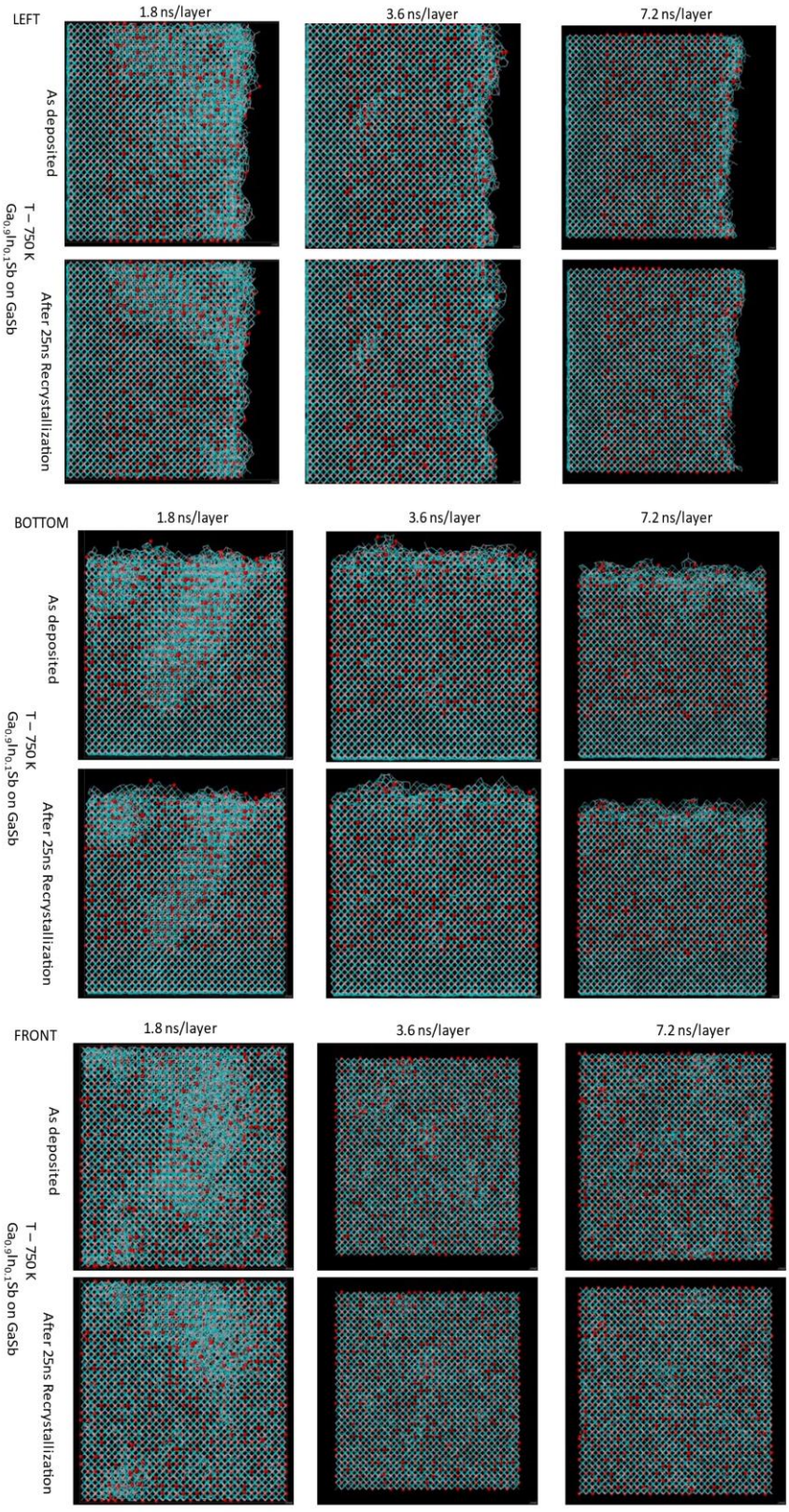

Figure 2: *10 Layer $Ga_{0.9}In_{0.1}Sb$ atop 3 layer GaSb substrate, 15x15 UC periodic cross section.*

case would point toward unrealistic crystalline stabilization due to some portion of the simulation protocols.

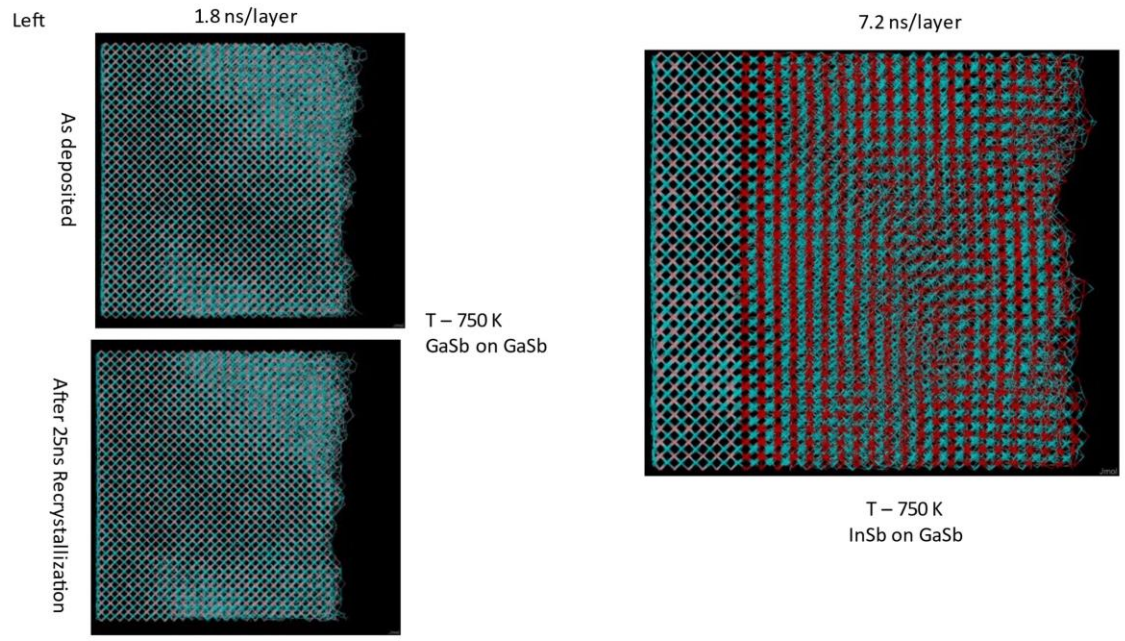

Figure 3: *Crystalline defects in rapidly deposited GaSb on GaSb and slowly deposited InSb on GaSb.*

Figure 3 presents the outcomes of these simulations, where substantial defected material is found in both cases. For the pure GaSb deposition on the GaSb substrate, this is an indicator that the misregistered region within the crystal is forming as a consequence of kinetic trapping of the system in an imperfect lattice configuration, and that care will have to be taken to ensure the deposition is occurring at rates that are slow enough to at least reasonably approximate the underlying thermodynamics of the system. In the case of the InSb deposition atop the GaSb substrate, the crystal is *also* defective, which at least points toward the fact that even at slower deposition rates, if the free energy differential of the lattice is large enough, we can expect the system to express this differential in a way that approximates the underlying physics of the system. In short, if we put material down too fast we can get a kinetically malformed system which cannot relax, but if we put material down slow enough, it does not look as likely that we will observe an overly stabilized crystal. This means we should be able to simulate a system that displays the appropriate equilibrium formation of dislocations and expect that explicitly seeded dislocations will remain stable enabling us to perform the simulations necessary to provide a basis for extracting thermodynamic terms for coarser grained approaches.

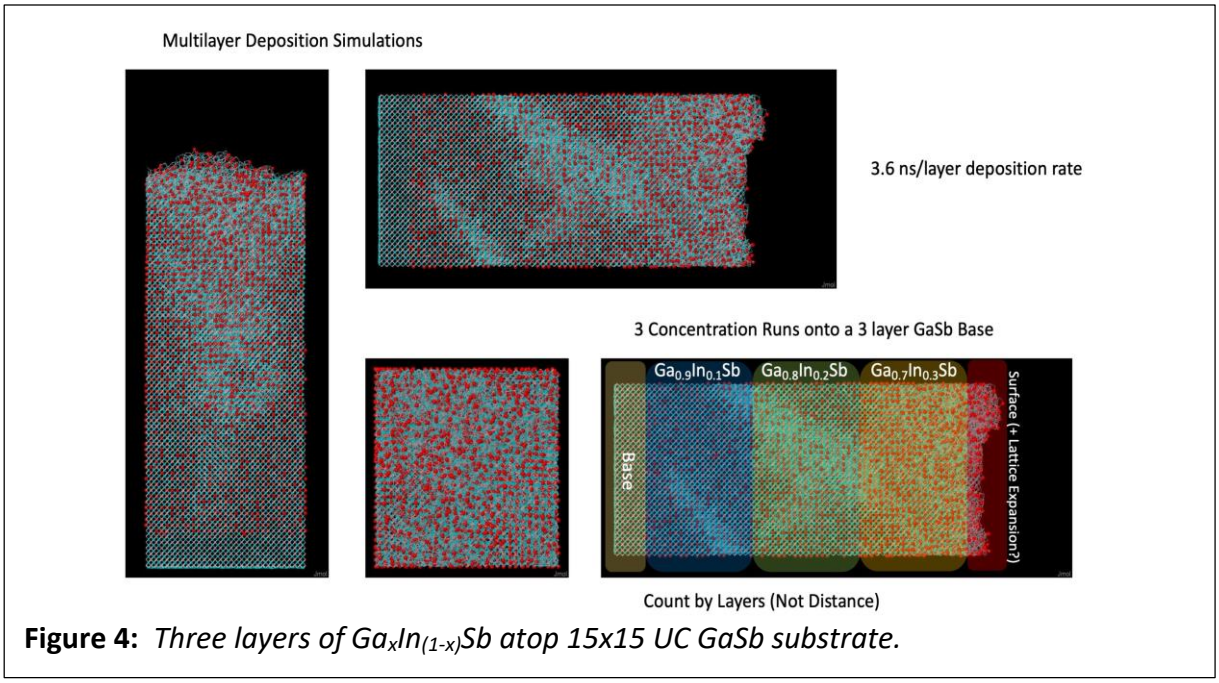

Figure 4: *Three layers of $Ga_xIn_{(1-x)}Sb$ atop 15x15 UC GaSb substrate.*

Next, we investigated the generation of a system with multiple concentration layers. Figure 4 shows a system with three layers of 10 unit cells each at 10% increasing concentrations deposited atop the standard 3 layer substrate with the previously investigated 15x15 UC cross-section. Here, initial investigation showed reasonable characteristics, including the formation of a dislocation region that essentially wraps through the periodic boundary conditions of the simulation cell, starting deep into the first deposited layer with composition $Ga_{0.9}In_{0.1}Sb$. More in-depth investigation of the defect structure shows that the dislocation starts within the first unit cell of the $Ga_{0.9}In_{0.1}Sb$ layer, leading to questioning of whether kinetic effects were still dominating the formation of defects. In order to try to answer these questions further, it was first necessary to determine a method of better visualizing the defects in the system than visual inspection. To this end, a literature search highlighted a myriad of potential schemes to automatically differentiate structural differences within a crystal. However, ultimately, we employed the Ovito[3] software package and it's implementation of the CNA type algorithm described by Maras *et. al.*[4] which effectively differentiates between zinc blende structured crystalline domains and wurtzite structured crystalline domains (i.e. cubic vs. hexatic crystal lattices). Figure 5 presents a picture of the crystal structure with these domains color coded as indicated.

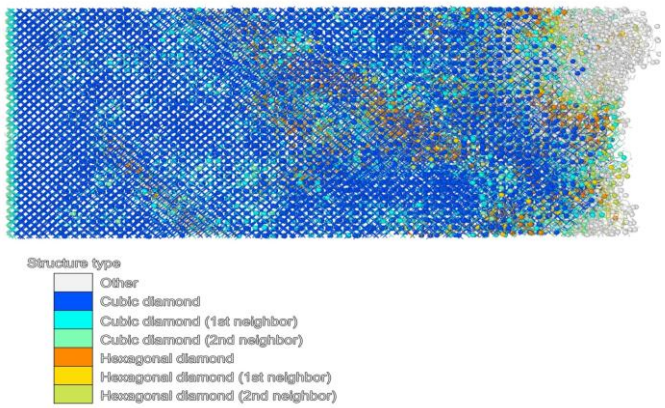

Figure 5: *CNA-type decomposition of crystalline environment of species in multilayer $Ga_xIn_{(1-x)}Sb$ stack.*

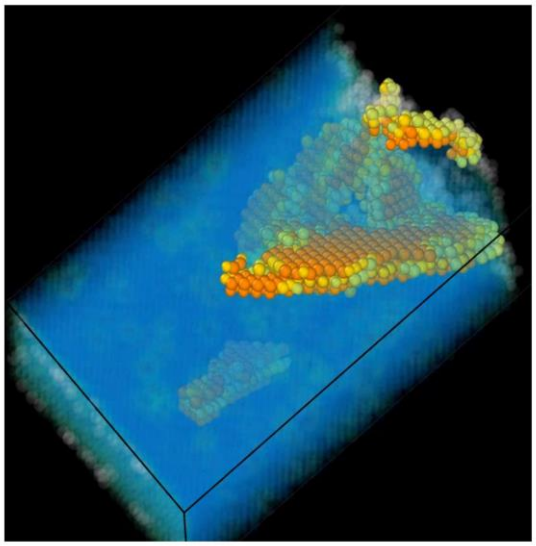

Figure 6: *Visualization of wurtzite structure regions (orange/yellow/green) embedded in standard zincblende background of $Ga_xIn_{(1-x)}Sb$ epitaxially layered crystal stack.*

One of the reasons the Ovito package was chosen was that it not only performed this analysis quickly and efficiently, but also provided significant control over the ability to personalize the manner in which the data is visualized. Hence, after substantial manipulation, it is possible to highlight only the wurtzite subset of the crystalline structure, allowing visualization of the defective volume as well as the edges of the dislocations which lead to the defective volume, as demonstrated in Figure 6.

Finally, in order to determine whether or not there are ancillary indicators associated with the presence of defect states, we used the defect state represented in Figure 6 to seed a stress calculation for the crystal with the same defect distribution. For this calculation, the virial pressure of each atom in the volume representing the nominal unit cells was averaged in 10 ps increments, yielding a time averaged stress tensor as a function of time for the system. These pressures were output every 100 ps, forming a movie showing the transition of the local stress tensors as a function of timing. In general, this movie demonstrates an underlying periodic rise and fall of localized stress, generally indicating the periodic nature of the stress in the system as phonons move through the crystal. However, atop these periodic pulsations of the local stress tensors are larger fluctuations in stress for cells occupied by the atoms within the dislocation planes imaged in Figure 6. Cells at various times from the movie thus produced are presented in Figure 7, to demonstrate the locations which are effectively low stress fluctuation and those which have higher degrees of fluctuation.

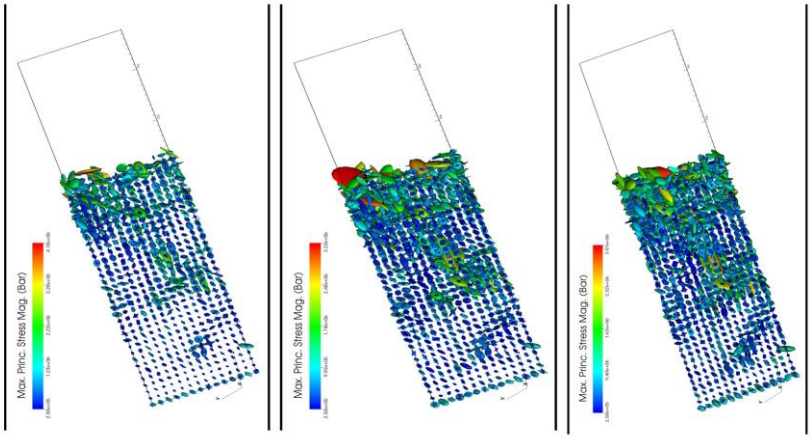

Figure 7: *Frames from stress tensor extraction showing that stress magnitudes are significantly higher in locations commensurate with dislocation features.*

2.3. Deposition Rate Investigation

Despite the increased ability to visualize the behavior of the system at multiple levels, there remained a fundamental question as to whether the simulation protocols were producing data which was sufficiently close to equilibrium to be useful. In order to try to definitively answer this question, we devised a series of simulations to thoroughly test the effect of both rates of deposition and alternative methods for equilibration involving advanced techniques available within LAMMPS. First, we conducted simulations across a variety of deposition times, from 1.8 ns /layer to 1440 ns/layer and conducted straight deposition runs for a system of $Ga_{0.5}In_{0.5}Sb$ across all these times. This composition was chosen under the assumption that it would have enough stress to have a base equilibrium free energy which favored dislocation formation, but also not so much mismatch between lattices that we expect no registration. Additionally, if one assumes ideal mixing between GaSb and InSb based on their pure volumes and the associated lattice parameter, this composition ought to be near the desired lattice parameter of 6.30 Å.

To probe equilibration quality for different dynamics approaches, we considered simulations across a complimentary axis to the simple lengthened deposition time. For these simulations, we chose the 144 ns/layer as our baseline rate. To compare so-called accelerated convergence techniques, we kept the total run time constant, but spent only 14.4 ns (10% of the total time) in deposition of the crystal layer, with the remaining 90% of the time reserved for relaxation. Relaxation occurred via one of two stochastic approaches: A simple substitutional Monte Carlo (SwapMC) scheme where after every 1 ps of simulation time, 1000 attempted identity exchanges are attempted between random atoms (as long as the atom swap WOULD exchange identities; no X->X swaps are allowed), where lowering energy is always accepted and raising energy is accepted based on the swap temperature which is kept equivalent to the simulation temperature (750K). The other approach incorporated time-stamped force-bias Monte Carlo (tfbMC), which essentially forces all atoms to move in the direction of their local energy gradient up to some maximum displacement (delta). There is no acceptance criteria here; instead the thinking is that as long as delta is chosen sufficiently small, the atoms will be forced to sample only within the local energy well, and once the environment becomes stable this distance limited sampling will ultimately converge to placing the atoms at their energetic minimum as the driving forces decay at least quadratically as the atoms approach their minimum energy configuration.

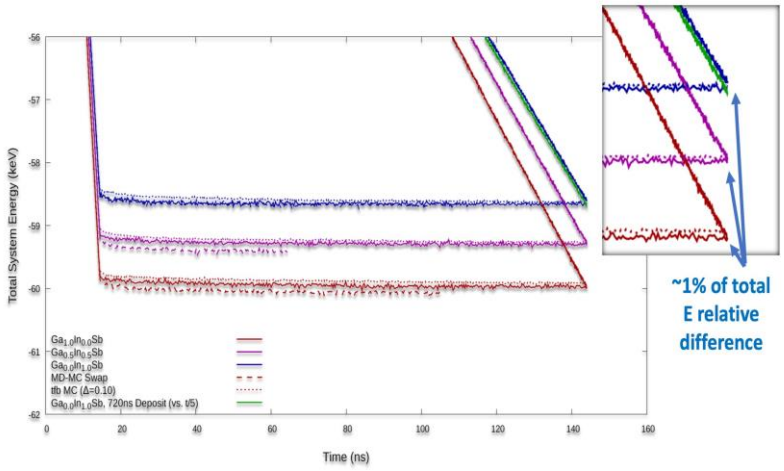

Figure 8: *Energy traces of various simulation/relaxation approaches over 144ns of total simulation time.*

Figure 8 presents the energy traces of these comparisons, with solid lines indicating the simple deposition over the entire time frame approach, dotted lines showing the tfbMC relaxation for 90% of the total time after deposition over the initial 10%, and dashed lines showing the SwapMC approach. As can be seen in Figure 8 by comparing the ending points (magnified in the inset) of the energy traces, all of the relaxation approaches are very similar after 144 ns of simulation time, with the relative orders of the techniques showing that $E_{SwapMC} < E_{Deposit} < E_{tfbMC}$. Although the nominal simulation time of all these approaches is 144ns, the pure 144ns deposition approach is the most efficient in terms of computational wall time since the MD deposition approach is less computationally intensive than either MC related technique. It's also important to note that either MC technique might benefit from attempting to optimize the MC step independent of the MD approach. However, given that tfbMC does the worst job of the three approaches and is the most expensive computationally, it is hard to justify spending the resources to optimize the MC portion of the compound simulation. In terms of the SwapMC approach, the only adjustable parameter is the number of swaps attempted, however lower number of swap attempts will necessarily drive the results back toward the pure MD calculation, while additional swap attempts will make the simulation run slower, and as the inset in Figure 8 demonstrates the remaining room to optimize the energy seems minimal compared to simply running pure deposition for the entire time. The latter seems particularly important given the fact that Figure 8 also demonstrates the energy trace for a system which deposits 10 times slower, with a notable result that the energy differential between a system which takes 144 ns/layer and one which takes 720 ns/layer is a very small energetic difference, implying an equally small structural deviation.

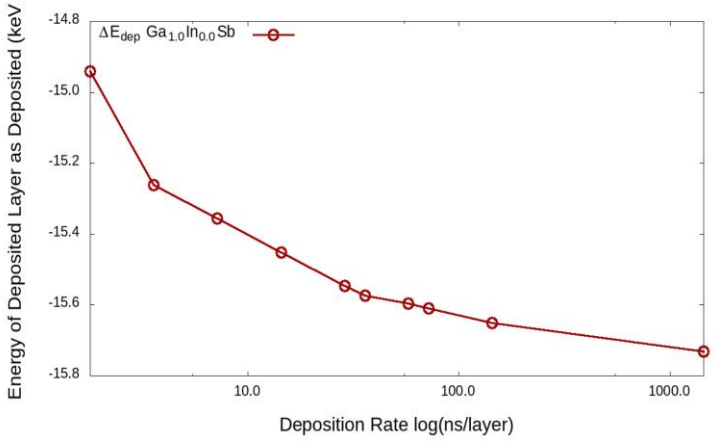

Figure 9: *Energy of single deposited layer vs. deposition time for the layer in pure MD deposition simulation approach.*

With respect to this latter observation, Figure 9 presents a graph which shows the energy as a function of deposition time per layer for a series of simulations which were all run as sole MD deposition simulations incorporating a single layer of deposition over the entire listed time. As can be seen, initial increases in deposition time lead to significant decrease in the overall layer energy, with very large differences in simulation time being required for very modest energetic changes past by the time the slower deposition times are reached. Interestingly, there seem to be multiple regimes being highlighted by the graph in Fig. 9, with the very fast simulation regime likely tapering off by roughly 3-5 ns/layer, an intermediate regime between this speed and 30-50 ns/layer, and then a long slow refinement regime for deposition rates > 50 ns/layer.

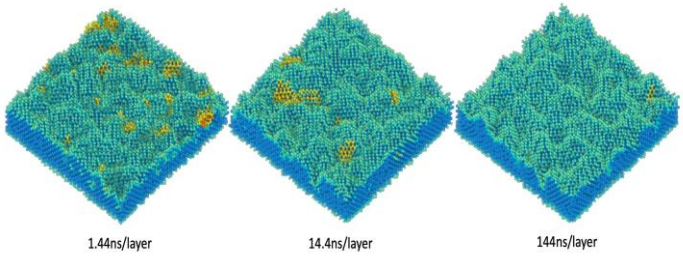

Figure 10: *Defects in 3 layers of Ga0.5In0.5Sb atop 3 layers of GaSb perfect substrate deposited at a rate of 144 ns/layer.*

While these energies are indicative of a correlation between increased crystal quality and increased deposition time, it is not a guarantee that this is the reason for the lower energies seen in Figure 9. For this reason, we present in Figure 10 pictures of three consecutive layers' worth of deposition at rates separated by two orders of magnitude. The most rapidly deposited layers (1.44 ns/layer) show an abundance of defect initiation sites, denoted by orange/yellow colored atoms. The intermediate deposition rate of 14.4 ns/layer shows fewer site locations for defects, although some of the defects have grown significantly larger in this case. Finally, the slowest deposition layer shows essentially a single defect growth in the rightmost corner. This slowest system was investigated extensively to characterize the behavior of the single defect highlighted in Figure 10. This defect was seen to appear/disappear multiple times over the course of deposition before finally stabilizing and becoming stationary. Similarly, other defects in other locations were also noted to appear, but eventually those defects were cleared as subsequent deposition and/or equilibration proceeded. Subsequent investigation of additional layer deposition for the 144 ns/layer system demonstrated further dislocation growth as the defective lattice was stabilized.

Additionally, further dislocations were formed over the course of the deposition of the next two layers, as shown in Figure 11. Here, the system has been rotated by 90 degrees counterclockwise in comparison to Figure 10, in order to more easily visualize the dislocation planes present. Figure 11 demonstrates that all the dislocations are of the 60° variety crossing the (110) plane in which the viewport resides. Additionally, the largest dislocation (and sole one present for 144 ns/layer in Figure 10) shows evidence of having a misfit dislocation resting along the <110> direction, located at the interfacial plane between the In augmented layer and the pure GaSb substrate. We also investigated the location of the dislocation formation, and attempted to correlate these locations with any structural features that were noteworthy at those locations in order to understand what caused the dislocations to form. The

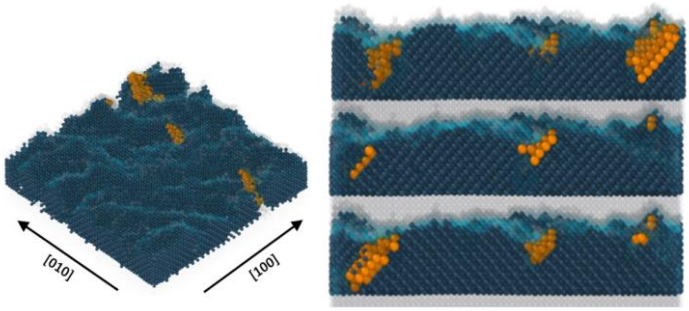

Figure 11: *Dislocation planes embedded in as-deposited $Ga_{0.5}In_{0.5}Sb$ at 144 ns/layer up to a nominal depth of 5 layers. Views of the 60° dislocations across (110) plane cuts looking in the* $[\bar{1}\bar{1}0]$ *direction.*

examples in Figure 12 show a strong correlation between the formation of these dislocations and locations where the uneven deposition of the epitaxial layers led to the formation of relatively deep wells in the height of the deposited layers. Figure 12a shows a top-down view of dislocation growth at each of the three dislocation sites noted, where it can be seen that there seems to be a correlation between the extra room provided by gaps in the underlying epitaxial layer coverage and the formation of increased stability wurtzite structured sites. If we look instead from the interface up through the layers, as in Figure 12b, we can see that there seems to be defect voids extending all the way to the interface of the epitaxial layers with the substrate which correspond to the location of the instigated dislocations. It should be noted that in these figures, for clarity, we image *only* the perfectly cubic or perfectly hexatic species present. This means, in turn, that the voids into which dislocation formation seeds are not actual voids with no crystalline material, but instead are persistent defects which disrupt some part of the neighbor structure necessary to achieve fully perfect zincblende or wurtzite structures. We have not yet analyzed the types of defects which occur in these "voids" to try to further refine our understanding of dislocation formation.

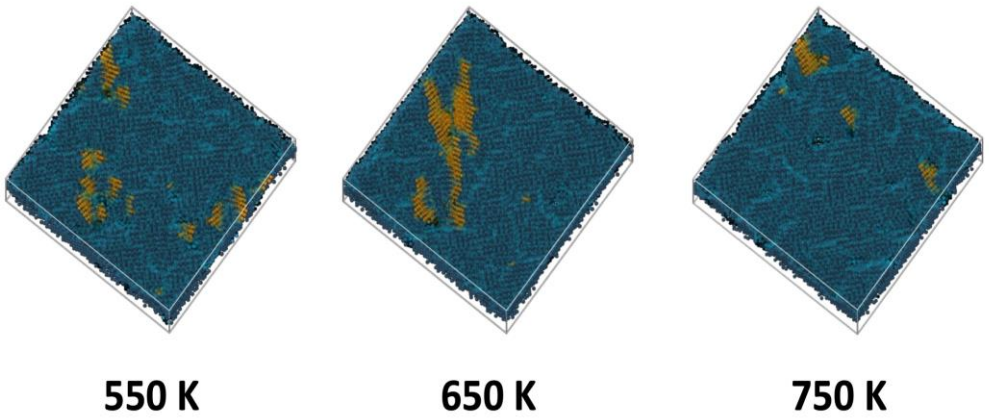

Figure 12: *Defect (orange) structures seen in 5 layer simulations of $Ga_{0.5}Sb_{0.5}In$ at 144 ns/layer and the indicated temperature.*

Ultimately, we were left with the following conclusions regarding this phase of our work:

1. Deposition at 144 ns/layer is likely slow enough to generate surface layers that are at or near enough to equilibrium to obtain useful information on dislocation generation.
2. We see the formation of 60° dislocations at points with defective crystallization that extends toward the surface layer. This would seem to be consistent with literature reports which state that 60° locations are seen from the impingement of separately deposited crystal regions as they grow together.
3. A 30x30 UC substrate is enough to establish multiplie independent dislocation seeds when deposition is sufficiently slow that relaxation to equilibrium of a nearby crystalline features is allowed.

2.4. Deposition Temperature Investigation

Finally, we have also briefly investigated the effect of simulation temperature on defect formation within our simulations. Previously, all simulations were run at 750K principally to provide the maximum energy to the system (while still maintaining reasonable crystal cohesion) because this allows the system to most easily approach equilibrium. Having achieved what we believe is a good approximant of equilibrium via our simulation approach, we then turned to running a select set of simulations at differing temperatures to ascertain what effect temperature reduction would have on the formation of dislocations within the system. As Figure 12 demonstrates, the effect of temperature is substantial.

Simulations were run for deposition of five layers of $Ga_{0.5}In_{0.5}Sb$ atop a 30x30 UC GaSb substrate, with a deposition rate of 144 ns/layer. Systems were started with the exact same substrate and same random seed, so the evolution of the structure is more directly relatable to the processing conditions approximated by the simulation. As can be seen, the systems at 550K and 650K exhibit significantly more defect structure than the system at 750K. However, it's hard to determine if there are any systematic trends in the system because both the 550K structure and 750K structure exhibit multiple small dislocated lattice regions, while the 650K system has seen significant aggregation and/or growth of a single massive region of dislocation with only one

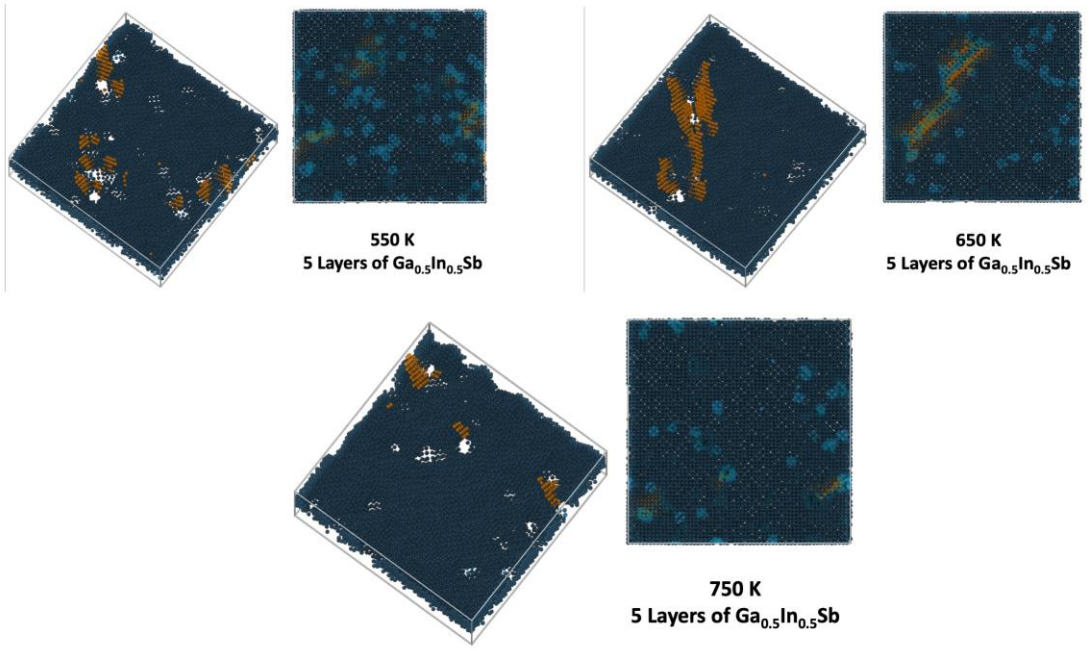

Figure 13: *In-depth view of the defect structure from Fig. 12 with non-perfectly coordinated atoms removed in the top down view and an "interface up" view showing the prominence of point defects at the interface.*

small additional ancillary defect. Figure 13 shows more in-depth pictures of the different temperature systems, with the angled overhead view having all non-perfect (i.e. fully zincblende

or wurtzite) atoms removed, as well as a bottom-up view of the deposited layers directly above the interfacial region. Here it becomes a bit easier to determine that there seems to be a systematic improvement in the quality of the layers as temperature increases.

In Figure 13, the top-down view of the three systems would seem to indicate a notable presence of layer-spanning "defects" (indicated in this method of depiction as blank 'holes') for the 550K system. Such visible 'holes' are seemingly less prevalent at 650K, before increasing again at 750K. However, by looking at the interface of the epitaxial layers with the underlying GaSb substrate in the right-hand pannels of Figure 13, a different story unfolds. In these figures, point defects representing the lack of fully perfected zincblende structure show as lighter blue circles. When investigating systematic trends from these pictures, the 550K system can be seen to have the most such defects, while the 650K system has perhaps slightly fewer but still a substantial amount. It is important to note for the 650K system the coalescence of these defects along the contour of the large, nearly-spanning dislocation present in the system. Finally, at 750K the presence of these defects is substantially diminished, indicating that at the highest temperature the system is able to crystallize notably better than at the lower temperatures, and providing a justification for the subsequent lesser amount of dislocations expressed in the top-down view. While each of these represents just a single instance of this type of observation and should be run again multiple times at each temperature in order to collect good statistical data, *it is gratifying to note that the systems behave in a manner consistent with experiment, where different regimes of epitaxial layer growth (isolated crystallite vs. spreading monolayers) have been observed in roughly commensurate temperature regimes*. In concert with the other investigations performed here, this points toward the ability of our simulation protocol and the potentials employed to allow for investigation of realistic physics in such systems, and would justify extending efforts to larger scale data collection and simulation systems for such data gathering.

3. Dislocation structure and evolution

3.1. Atomistic Identification of Dislocations

Given the ultimate goal of understanding and guiding the evolution of dislocations to minimize their effect on desirable electronic properties, a necessary first step is understanding the types of dislocations formed in the $Ga_xIn_{1-x}Sb$ system. While these answers are generally available from the literature for the general case of III-V semiconductors, the specific system under investigation is poorly represented in such literature, as investigations are (understandably) carried out on simpler tertiary systems, such as the simulated $GaSb/Ga_{0.5}In_{0.5}Sb$ system discussed above. Having produced systems we feel adequately represent reality as detailed above, we then turned to investigation of the dislocation structure(s) present in such system. Figures 14-16 present the results of employing the dislocation extraction algorithm[5] on our simulated systems, to characterize the types of dislocations formed in the 550K-750K samples. While the lower temperature samples showed sufficient dislocation structure to be of interest evolved within the first 5 layers of simulation, the 750K simulation required deposition of additional layers (8 total) before significant dislocation structure appeared.

Figure 14 shows the evolved dislocation structure of the 550K system, which is dominated by the presence of multiple stacking faults (SF) related dislocations, which subsequently merge into Lomer-Cottrell (LC) dislocations. The third area of stacking faults with only $\vec{b}$ of type $1/6\langle 112\rangle$ dislocations and the unidentified red dislocation presented in Figure 14 represents the dislocation at the top portion of the 550K image in Figure 13. The lack of LC dislocations in this area of defects is due to the fact that both stacking faults remain parallel to one another, preventing the intersection and pinning of the defect into a LC dislocation under the simulation time thus far expressed.

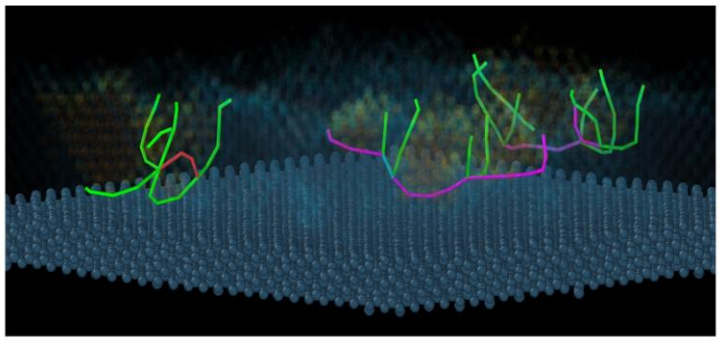

Figure 14: *Dislocation structure in the 550K deposition of 5 layers of $Ga_{0.5}In_{0.5}Sb$ atop a GaSb substrate (dark blue spheres). Green lines are stacking faults with $\vec{b}$ of type $1/6\langle 112\rangle$, magenta are Lomer-Cottrell dislocations with $\vec{b}$ of type $1/6\langle 110\rangle$, and red are dislocation lines of an unidentified $\vec{b}$, likely due to bulk packing disruptions near the surface.*

Figure 15 shows the dislocation structure of the 650K system, where the system is dominated by two large scale dislocation regions. Here, since the LC dislocations are immobile, it would be unexpected for the dislocations to merge despite the fact that a pure atomistic view indicates that the system might simply be waiting to undergo perfection of an underlying misfit dislocation. Such analysis shows the utility of investigating the system from a dislocation oriented viewpoint as well as the atomistic.

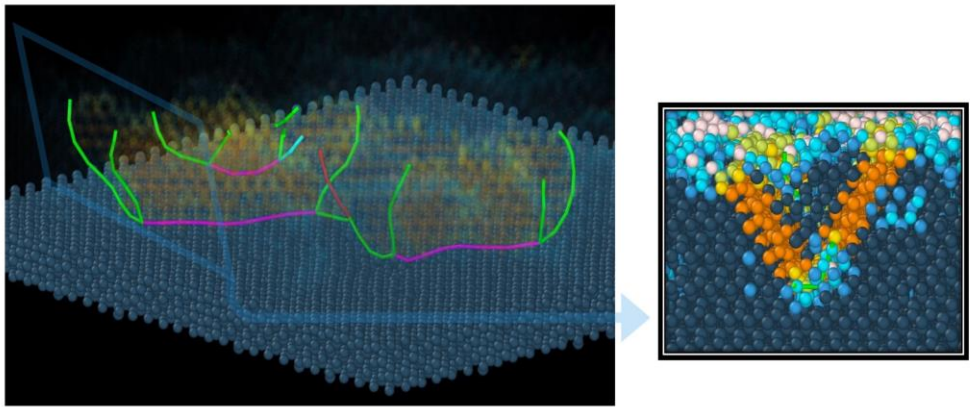

Figure 15: *Dislocation structure in the 650K deposition of 5 layers of Ga0.5In0.5Sb atop GaSb substrate. Colors of lines have the same meaning as in Fig. 14. The extract shows the double Lomer-Cottrel stack visible in the main picture (looking roughly along the LC dislocation lines) highlighting the mis-stacked region of hexatic material.*

Finally, Figure 16 shows the dislocation network formed for the 750K simulation. As mentioned previously, no notable dislocation structure was present in the first 5 layer deposition run of the 750K system, so an extended run consisting of 8 layers of material was instead analyzed. Here, there is a notable predominance of SF dislocations, yet a paucity of LC pinnings of these faults deeper within the crystal. Instead, at 750K we see the emergence of perfect dislocations which should be mobile enough to eventually exit the crystal. It may be that such dislocations are seen because the increased temperature of the simulation allows for easier rearrangement of stacking faults at the surface before they get "frozen in" by deposition of the next layer. Such a mechanism if present would likely be not only temperature dependent, but concentration dependent as well, as stabilization and mobility of stacking fault related dislocations would likely depend upon the local concentration.

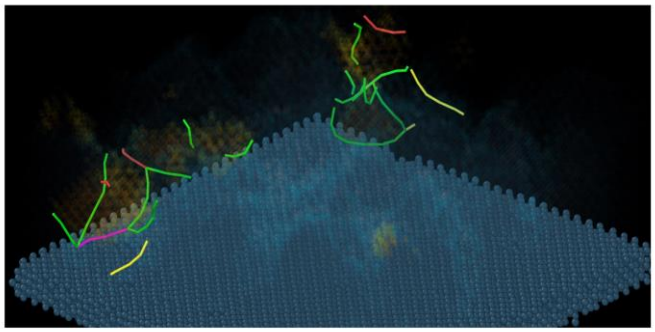

Figure 16: *Dislocation structure in the 750K deposition of 8 layers of Ga0.5In0.5Sb atop GaSb substrate. Colors of lines have the same meaning as in Fig. 14, with the additional yellow color lines representing "perfect" FCC dislocations with* $\vec{b}\ of\ type\ 1/2\langle 110\rangle$.

3.2. Linking to Larger Dislocation Structures

Ultimately, to understand the dynamics of dislocation evolution, we need to marry the understanding of individual dislocations provided via MD simulations with the collective dislocation interactions which become tractable when employing the technology of discrete dislocation dynamics (DDD). In DDD, the material is simulated in an abstract sense by extracting all portions of the bulk material which represent an imperfect crystal, and simulating only the interactions of the dislocations embedded within the otherwise presumed perfect crystal. Essentially, DDD allows for the visualization employed in Figures 15-16 to instead represent the underlying dynamics of the system, by discretizing and evolving dislocation lines pursuant to the controlling laws of linear elasticity. To accomplish this, DDD maps the motion of the dislocation lines as discrete dislocation line segments which interact with the elastic continuum of the perfect background crystal. In the limit of isolated dislocation segments and uniform bulk material, this mapping is relatively straightforward via the employment of linear elastic theory. Instead, the difficulty comes in when considering the interactions of dislocations which are close enough to one another that their localized stress distortions over the nearby crystal begin to interact. In such cases, the tenets of linear elastic theory become increasingly incapable of prediction, since the specifics of such interactions are ultimately mediated by the non-continuous nature of the atomic-based interactions between nearby crystal defects. This is where the linkage between atomic level simulations and the DDD continuum simulations becomes critical. Utilizing atomic simulations, it is possible to understand the way in which two dislocations with differing character interact by simulating those dislocations at a series of interaction distances and extracting effective potentials and/or energies for parameterization of the DDD interactions.

Having established the reliability of the MD simulations to provide parameterization information for the DDD simulations, the following list of information needs to now be generated for inclusion in continuum simulations:

- Elastic and lattice constants for perfect crystals of $Ga_xIn_{(1-x)}Sb$ across graded values of x (Initial steps of x += 0.10) as well as at the interfaces between two subsequent gradations
- Dislocation mobility as a function of concentration, temperature, and stress

Given the two sets of differing calculations above, initial parameterization of the DDD simulations may be moved forward. It should be noted that the second item represents a large number of simulations (requiring essentially a simulation for a variety of stresses and at least a few temperatures across the differing dislocation line/Burger vector combination for reasonable stresses expected due to localized distortions and/or interfacial effects in the graded layer). However, unlike the previous simulations performed, these simulations are not stochastic in nature, but instead represent more deterministic calculations with prescribed initial geometries and loading conditions. While such simulations will require substantial computational time, they should not require the amount of trial, error, and adjustment that previous simulations have. We will employ state of the art tools and research such as the dislocation simulation toolkit recently developed[6] to ease the burden of setting up appropriate systems and reduce the calculations to ones which are more easily manageable.

Our current plans are to employ the ParaDIS massively parallel DDD simulation package to perform the simulations. Inasmuch as much of the recent DDD capabilities discussed and relied upon in the literature have been enabled by the work of Wei Cai, who is also associated with ParaDIS, the expectation is that incorporation of the data generated using techniques outlined by Prof. Cai's for marrying simulation and DDD[7] should be straightforward.

---

[1] A. J. Ciani, C. H. Grein, B. Irick, M. Miao, N. Kioussis, *Opt. Eng.* **56** 091609 (2017).
[2] A. P. Thompson, H. M. Aktulga, R. Berger, D. S. Bolintineanu, W. M. Brown, P. S. Crozier, P. J. in 't Veld, A. Kohlmeyer, S. G. Moore, T. D. Nguyen, R. Shan, M. J. Stevens, J. Tranchida, C. Trott, S. J. Plimpton, *Comp. Phys. Comm.*, **271** 10817 (2022).
[3] A. Stukowski, *Modelling Simul. Mater. Sci. Eng.* **18** 015012 (2010).
[4] E. Maras, O. Trushin, A. Stukowski, T. Ala-Nissila, H. df
[5] A. Sutkowski, K. Able, *Modelling Simul. Mater. Sci. Eng.* **18** 085001 (2010).
[6] Z. Pei, *Comp. Phys. Comm.* **233** 44 (2018).
[7] J. Chang, W. Cai, V. V. Bulatov, S. Yip, *Comp. Mater. Sci.* **23** 111 (2002).